

From Current to Constituent Quarks: a Renormalization Group Improved Hamiltonian-based Description of Hadrons.

Adam P. Szczepaniak and Eric S. Swanson

Department of Physics, North Carolina State University, Raleigh, North Carolina 27695-8202

Abstract

A model which combines the perturbative behavior of QCD with low energy phenomenology in a unified framework is developed. This is achieved by applying a similarity transformation to the QCD Hamiltonian which removes interactions between the ultraviolet cutoff and an arbitrary lower scale. Iteration then yields a renormalization group improved effective Hamiltonian at the hadronic energy scale. The procedure preserves the standard ultraviolet behavior of QCD. Furthermore, the Hamiltonian evolves smoothly to a phenomenological low energy behavior below the hadronic scale. This method has the benefit of allowing radiative corrections to be directly incorporated into nonperturbative many-body techniques. It is applied to Coulomb gauge QCD supplemented with a low energy linear confinement interaction. A nontrivial vacuum is included in the analysis via a Bogoliubov-Valatin transformation. Finally, the formalism is applied to the vacuum gap equation, the quark condensate, and the dynamical quark mass.

I. INTRODUCTION

There is currently an unfortunate dichotomy in analytical approaches to QCD. One either calculates using Lagrangian methods and, with the exception of Monte Carlo simulations, is limited to perturbative calculations, or one employs low energy models of QCD and eschews the known high energy behavior of the theory. There are only a few approaches where, for example, the calculation of hadronic form factors may be connected to the expected quark counting behavior at high energies. These include QCD sum rules [1], NRQCD [2], and to some extent light cone quantization [3]. This paper develops a formalism by which the known high energy behavior of QCD (pQCD) may be rigorously joined to standard phenomenological models of hadrons. This is achieved by using the renormalization group to run the scale of the QCD Hamiltonian to the hadronic regime where it smoothly joins a fixed phenomenological behavior.

This approach imposes important constraints on the low energy portion of the model. If one wishes to recover pQCD, one must work with current quarks. Thus the low energy theory must also deal with current quarks. However phenomenology indicates that constituent quarks are the relevant degrees of freedom at low energy. Thus, one must allow for spontaneous chiral symmetry breaking in the model. This, in turn, means that a nontrivial vacuum must be incorporated into the theory. Finally, we see that one must use many-body techniques when calculating observables. The Hamiltonian-based renormalization group we employ is particularly useful in this regard because it allows for the use of nonperturbative many-body techniques.

We call this approach the “Dynamical Quark Model” (DQM). The fact that the low energy behavior of the DQM evolves directly from pQCD is very helpful when analyzing the dynamical structure of the low energy portion of the model. For example, we are able to rigorously establish that the non-Abelian Coulomb interaction is responsible for the quark structure of confinement in the heavy quark limit. We are also able to resolve ambiguities in the separation of short and long distance phenomena when evaluating current matrix

elements.

This brings us to a final important reason for employing the renormalization group improved (RGI) Hamiltonian. As stated, we are obliged to use many-body methods while working with the model. The major tools at our disposal are the Tamm-Dancoff approximation (TDA) and the random phase approximation (RPA). These build, for example, meson bound states of the type $q\bar{q}$ or $q\bar{q} + q\bar{q}(q\bar{q}\bar{q}) + \dots$ respectively. If one wants to allow for mixing to, for example, $q\bar{q}g$ or $qq\bar{q}\bar{q}$ states then these must be explicitly included in the calculation. Such coupled channel problems are rather difficult to solve. Thus it is imperative to include as much of the physics of Fock sector mixing as possible directly into the Hamiltonian. For example, the phenomenologically important hyperfine splittings can be incorporated by iterating the $q\bar{q}g$ vertex, thereby adding an effective transverse gluon exchange operator to the Hamiltonian. Using the RGI Hamiltonian automatically achieves this goal.

The remainder of this paper is organized as follows. A model based on the Coulomb gauge QCD Hamiltonian is introduced in Section II and its high energy behavior is analyzed. To do this we impose a chiral invariant regulator and then calculate the RGI Hamiltonian. The counter-term structure and possible perturbative and nonperturbative renormalization schemes are then discussed. In Section III we show how effective operators are constructed and examine the ultraviolet behavior of the quark creation operator, the axial current, and the scalar quark density. Section IV presents nonperturbative, one-loop, many-body calculations of the vacuum gap equation, the quark condensate, and the dynamical quark mass. We summarize and conclude in Section V.

II. THE EFFECTIVE HAMILTONIAN

Our starting point will be the Coulomb gauge Hamiltonian of QCD. There are many reasons for choosing to work in the Coulomb gauge. For example, as stated in the Introduction, it is expedient to have explicit $\bar{q}q$ interactions in the Hamiltonian to make a connection

with quark model phenomenology. Further advantages of the Coulomb gauge are that all unphysical degrees of freedom have been eliminated so that subsidiary conditions on states are not necessary. This also implies that the norm is positive definite. Furthermore, spurious retardation effects are minimized.

We note that it is impossible to address the issue of gauge invariance in this model because it is defined in a specific gauge. However, QCD is gauge invariant so it is perfectly acceptable to work in a fixed gauge. The real issue is not how the model changes under a gauge transformation, but how well the phenomenological low energy interaction V_{conf} we will use mimics the actual low energy behavior of QCD. The only way to address this is to solve QCD (on the lattice, say) or to compare the predictions of the model to observables. This will be the subject of future papers. For now, we note that lattice gauge theory indicates that V_{conf} should be a linear potential when the quarks are static, our predicted glueball spectrum agrees well with lattice calculations [4], and the model is guaranteed to reproduce the success of the naive quark model for heavy quarks.

The DQM Hamiltonian is obtained after a rather long series of operations. The first step is to regulate the bare Hamiltonian in a manner which is consistent with the renormalization scheme we shall employ and which does not interfere with the nonperturbative calculations we will eventually perform. This introduces a scale into the Hamiltonian which we shall call Λ_0 . Renormalization is carried out by performing a similarity transformation on the Hamiltonian. This transformation is designed to eliminate couplings between the scale Λ_0 and an arbitrary, but nearby, lower scale Λ_1 . The similarity transformation preserves the spectrum of the Hamiltonian (to the order we work to) while restricting the matrix elements of the Hamiltonian to a smaller, band-diagonal form. Since elimination of these couplings reveals UV divergences in the bare Hamiltonian the third step is to absorb these by fixing appropriate counter-terms. After this we repeat the last two steps above, thereby generating a renormalization group improved effective Hamiltonian. The final step of our program is to include a phenomenological term which is meant to model the behavior of the higher order terms that have been ignored in the perturbative analysis.

A. Model Definition

As mentioned above, our starting point is the Coulomb gauge Hamiltonian of QCD [5],

$$H = H_0 + V, \quad (1)$$

where H_0 is the free Hamiltonian,

$$H_0 = \int d\mathbf{x} \psi(\mathbf{x})^\dagger [-i\boldsymbol{\alpha} \cdot \boldsymbol{\nabla} + \beta m] \psi(\mathbf{x}) + Tr \int d\mathbf{x} [\boldsymbol{\Pi}^2(\mathbf{x}) + \mathbf{B}_{\mathcal{A}}^2(\mathbf{x})]. \quad (2)$$

The degrees of freedom are the transverse gluon field $\mathbf{A} = \mathbf{A}^a T^a$, its conjugate momentum $\boldsymbol{\Pi}$, and the quark field in Coulomb gauge. We have represented the Abelian portion of the non-Abelian magnetic field by $\mathbf{B}_{\mathcal{A}}$. The interactions are given by

$$\begin{aligned} V = & Tr \int d\mathbf{x} [\mathcal{J} \boldsymbol{\Pi}(\mathbf{x}) \mathcal{J}^{-1} \boldsymbol{\Pi}(\mathbf{x}) - \boldsymbol{\Pi}^2(\mathbf{x})] + Tr \int d\mathbf{x} [\mathbf{B}^2(\mathbf{x}) - \mathbf{B}_{\mathcal{A}}^2(\mathbf{x})] \\ & + \frac{1}{2} g^2 \int d\mathbf{x} d\mathbf{y} \mathcal{J}^{-1} \rho^a(\mathbf{x}) \langle \mathbf{x}, a | (\boldsymbol{\nabla} \cdot \mathbf{D})^{-1} (-\boldsymbol{\nabla}^2) (\boldsymbol{\nabla} \cdot \mathbf{D})^{-1} | \mathbf{y}, b \rangle \mathcal{J} \rho^b(\mathbf{y}) \\ & - g \int d\mathbf{x} \psi^\dagger(\mathbf{x}) \boldsymbol{\alpha} \cdot \mathbf{A}(\mathbf{x}) \psi(\mathbf{x}) \end{aligned} \quad (3)$$

where $\mathcal{J} = \text{Det}[\boldsymbol{\nabla} \cdot \mathbf{D}]$, $\mathbf{D} = \boldsymbol{\nabla} - g\mathbf{A}$, is the covariant derivative in the adjoint representation and $\mathbf{B} = B_i = \nabla_j A_k - \nabla_k A_j + g[\mathbf{A}_j, \mathbf{A}_k]$.

The density, ρ , in the non-Abelian Coulomb interaction is the full QCD color charge and thus has both quark and gluonic components,

$$\rho^a(\mathbf{x}) = \psi^\dagger(\mathbf{x}) T^a \psi(\mathbf{x}) + f^{abc} \mathbf{A}^b(\mathbf{x}) \cdot \boldsymbol{\Pi}^c(\mathbf{x}). \quad (4)$$

B. The Similarity Renormalization Scheme

An effective Hamiltonian is defined to be an operator which, when acting within a subspace of the original Hilbert space, yields the same observables as the original Hamiltonian. Usually the effective Hamiltonian is constructed by dividing the Hilbert space into two portions which are defined by projection operators, P , and $Q = 1 - P$. In general the effective

Hamiltonian may be written as a sum of the projected Hamiltonian, PHP and a set of effective interactions, V_{eff} arising from elimination of couplings between the P and Q spaces. Typical methods for constructing the effective Hamiltonian produce energy denominators in V_{eff} which may vanish. This introduces severe complications when attempting to nonperturbatively diagonalize the effective Hamiltonian. An elegant way for avoiding these problems is given by the similarity transformation scheme of Glazek and Wilson [6].

The scheme involves ordering the states according to their free energy levels. The interaction part of the Hamiltonian is then regulated by ignoring matrix elements with free energy differences which are greater than Λ_0 . One then proceeds by constructing a similarity transformation which removes the couplings between states whose energy differences lie between Λ_0 and Λ_1 . This procedure generates an effective potential which incorporates the eliminated physics.

We start by constructing the eigenstates of the free Hamiltonian, H_0 , by expanding the quark and gluon field operators in normal modes,

$$\psi(\mathbf{x}) = \sum_{\tau} \int \frac{d\mathbf{k}}{(2\pi)^3} (u(\mathbf{k}, \tau) b(\mathbf{k}, \tau) + v(-\mathbf{k}, \tau) d^{\dagger}(-\mathbf{k}, \tau)) e^{i\mathbf{k}\cdot\mathbf{x}} \quad (5)$$

$$\mathbf{A}(\mathbf{x}) = \sum_a \int \frac{d\mathbf{k}}{(2\pi)^3} \frac{1}{\sqrt{2\omega(\mathbf{k})}} (\mathbf{a}(\mathbf{k}, a) + \mathbf{a}^{\dagger}(-\mathbf{k}, a)) e^{i\mathbf{k}\cdot\mathbf{x}}. \quad (6)$$

The quark operators are given in the helicity basis and all discrete quantum numbers (helicity, color and flavor, for the quarks and color for the gluons) are collectively denoted by τ and a respectively. Note the use of non-relativistic normalization so that, $u^{\dagger}u = v^{\dagger}v = 1$, and

$$\{b(\mathbf{k}_1, \tau_1), b^{\dagger}(\mathbf{k}_2, \tau_2)\} = \{d(-\mathbf{k}_1, \tau_1), d^{\dagger}(-\mathbf{k}_2, \tau_2)\} = (2\pi)^3 \delta(\mathbf{k}_1 - \mathbf{k}_2) \delta_{\tau_1, \tau_2} \quad (7)$$

and

$$[\mathbf{a}(\mathbf{k}_1, a_1), \mathbf{a}^{\dagger}(\mathbf{k}_2, a_2)] = (2\pi)^3 \delta(\mathbf{k}_1 - \mathbf{k}_2) (\mathbf{1} - \hat{\mathbf{k}}_1 \hat{\mathbf{k}}_1) \delta_{a_1 a_2}. \quad (8)$$

The free Hamiltonian is then given by,

$$H_0 = \sum_{\tau} \int \frac{d\mathbf{k}}{(2\pi)^3} E(\mathbf{k}) [b^{\dagger}(\mathbf{k}, \tau)b(\mathbf{k}, \tau) + d^{\dagger}(\mathbf{k}, \tau)d(\mathbf{k}, \tau)] + \sum_a \int \frac{d\mathbf{k}}{(2\pi)^3} \omega(\mathbf{k}) \mathbf{a}^{\dagger}(\mathbf{k}, a) \mathbf{a}(\mathbf{k}, a) \quad (9)$$

where $E(\mathbf{k}) = \sqrt{m^2 + \mathbf{k}^2}$, $\omega(\mathbf{k}) = |\mathbf{k}|$ and we have dropped the constant, zero point energy.

In the basis of eigenstates of H_0 , $H_0|n\rangle = E_n|n\rangle$, the cut-off method of Glazek and Wilson may be written as

$$\langle m|H|n\rangle \rightarrow \langle m|H^{\Lambda_0}|n\rangle = E_n \delta_{nm} + f_{mn}(\Lambda_0) \langle m|V|n\rangle. \quad (10)$$

Here $f_{mn}(\Lambda_0)$ is a function which is unity for $|E_{mn}| << \Lambda_0$ and zero for $|E_{mn}| >> \Lambda_0$ (we have defined $E_{mn} = E_m - E_n$). For our purposes we find it convenient to use a sharp cut-off,

$$f_{mn}(\Lambda_0) = \theta(\Lambda_0 - |E_{mn}|). \quad (11)$$

In this paper we will study only the quark sector of the Hamiltonian. Thus all gluon interactions will be ignored except those which contribute to effective quark operators. A discussion of the gluonic sector has been given in Ref. [4], where it has been successfully applied to the glueball spectrum. The effort in deriving effective operators in the gluon sector is currently in progress [7].

The operators of the bare regulated Hamiltonian contributing to order g^2 in the quark sector are,

$$V^{\Lambda_0} = gV_1^{\Lambda_0} + g^2V_2^{\Lambda_0} \quad (12)$$

where

$$V_1^{\Lambda_0} = \sum_{\tau_1 \tau_2 a} \int \frac{d\mathbf{k}_1}{(2\pi)^3} \frac{d\mathbf{k}_2}{(2\pi)^3} \frac{d\mathbf{l}}{(2\pi)^3} \delta(\mathbf{k}_1 - \mathbf{k}_2 - \mathbf{l}) \frac{T_{12}^a}{\sqrt{2\omega(\mathbf{l})}} \left[[u_1^{\dagger} \boldsymbol{\alpha} u_2] \theta(\Lambda_0 - |E(\mathbf{k}_2) + \omega(\mathbf{l}) - E(\mathbf{k}_1)|) b^{\dagger}(\mathbf{k}_1, \tau_1) b(\mathbf{k}_2, \tau_2) \mathbf{a}(\mathbf{l}, a) + \dots \right] \quad (13)$$

and

$$\begin{aligned}
V_2^{\Lambda_0} = & \sum_{\tau_1 \dots \tau_4} \int \frac{d\mathbf{k}_1}{(2\pi)^3} \frac{d\mathbf{k}_2}{(2\pi)^3} \frac{d\mathbf{k}_3}{(2\pi)^3} \frac{d\mathbf{k}_4}{(2\pi)^3} V_c(\mathbf{k}_1 - \mathbf{k}_2) \delta(\mathbf{k}_1 + \mathbf{k}_2 - \mathbf{k}_3 - \mathbf{k}_4) T_{13}^a T_{24}^a \\
& \times \left[\theta(\Lambda_0 - |E(\mathbf{k}_3) + E(\mathbf{k}_4) - E(\mathbf{k}_1) - E(\mathbf{k}_2)|) [-u_1^\dagger u_3][u_2^\dagger u_4] \right. \\
& \left. b^\dagger(\mathbf{k}_1, \tau_1) b^\dagger(\mathbf{k}_2, \tau_2) b(\mathbf{k}_3, \tau_3) b(\mathbf{k}_4, \tau_4) + \dots \right]. \tag{14}
\end{aligned}$$

In V_1 and V_2 the ellipses denote an additional seven and fifteen terms respectively and V_c is the momentum space Coulomb potential. The additional terms correspond to interactions involving all possible permutations of quark and antiquark operators. The subscripts on the spinors and the Gell-Mann matrices refer to indices of the appropriate quark operators. Normal ordering the bare Hamiltonian with respect to the perturbative basis generates a new one body operator given by

$$\begin{aligned}
g^2 V_{self.C} = & \sum_{\tau} \int \frac{d\mathbf{k}}{(2\pi)^3} \left[\Sigma_C(\mathbf{k}; \Lambda_0^C) [b^\dagger(\mathbf{k}, \tau) b(\mathbf{k}, \tau) + d^\dagger(-\mathbf{k}, \tau) d(-\mathbf{k}, \tau)] \right. \\
& \left. + \theta\left(\frac{\Lambda_0}{2} - E(\mathbf{k})\right) G_C(\mathbf{k}; \Lambda_0^C) [b^\dagger(\mathbf{k}, \tau) d^\dagger(-\mathbf{k}, \tau) + d(-\mathbf{k}, \tau) b(\mathbf{k}, \tau)] \right]. \tag{15}
\end{aligned}$$

Both Σ_C and G_C (which are given in the Appendix) are divergent and not regulated by Λ_0 . In Eq. [15] they have been regulated individually with a cutoff denoted by Λ_0^C . Since all divergences of the bare Hamiltonian are to be absorbed by counter-terms one could subtract this self energy in its entirety and simply ignore it. However we shall show subsequently that covariance requires that a portion of $V_{self.C}$ be maintained in the Hamiltonian. The $O(g^2)$ bare potential will therefore be given by,

$$V^{\Lambda_0}(\Lambda_0^C) = g V_1^{\Lambda_0} + g^2 V_2^{\Lambda_0} + g^2 V_{self.C}^{\Lambda_0}(\Lambda_0^C) \tag{16}$$

where we have made the Λ_0 and Λ_0^C dependence explicit. The Λ_0 dependence of $V_{self.C}$ arises only from the term proportional to G_C since Σ_C is diagonal in the perturbative basis and therefore, according to Eq. [10], is Λ_0 independent. So long as the ratio Λ_0^C/Λ_0 remains finite as both scales approach infinity, the existence of a second scale will be irrelevant (to the order to which we work). From now on we will set $\Lambda_0^C = \Lambda_0$.

We are now ready to calculate the equivalent of the P -space Hamiltonian, $PHP = H^{\Lambda_1}$

and of the effective Hamiltonian, $H_{eff}^{\Lambda_1}$. The matrix elements of the former are defined using Eq. [10],

$$\langle m | H^{\Lambda_1} | n \rangle = E_n \delta_{nm} + f_{mn}(\Lambda_1) \langle m | V | n \rangle, \quad (17)$$

where V depends on Λ_0 (and Λ_0^C in general) as discussed above. Since within the P -space the spectrum of the bare Hamiltonian and that of the effective Hamiltonian are to be identical, we may write

$$H_{eff}^{\Lambda_1} = S H^{\Lambda_0} S^{-1} \quad (18)$$

where S is a unitary matrix such that matrix elements, $\langle m | H_{eff}^{\Lambda_1} | n \rangle$ are nonzero only within the P -space, i.e. for states that satisfy

$$|E_{nm}| < \Lambda_1. \quad (19)$$

To construct S we proceed by expanding it in powers of the strong coupling

$$S = e^{iR}, \quad (20)$$

and

$$R = gR_1 + g^2R_2 + \mathcal{O}(g^3). \quad (21)$$

Then

$$\begin{aligned} H_{eff}^{\Lambda_1} = & H_0 + g(V_1 + i[R_1, H_0]) \\ & + g^2 \left(V_2 + V_{self.C} + i[R_2, H_0] + i[R_1, V_1] - \frac{1}{2}[R_1, [R_1, H_0]] \right) + \mathcal{O}(g^3). \end{aligned} \quad (22)$$

Here, the dependence of the V 's on Λ_0 is implicit. To order g , $ig[R_1, H_0]$ is chosen to eliminate matrix elements of gV_1 between the scales Λ_1 and Λ_0 . Thus, to this order, one need simply replace the two terms in the first brackets with $V_1^{\Lambda_1}$,

$$\langle m | V_1^{\Lambda_1} | n \rangle = \theta(\Lambda_1 - |E_{mn}|) \langle m | V_1 | n \rangle. \quad (23)$$

Similarly, to order g^2 , $ig^2[R_2, H_0]$ eliminates all matrix elements of the expression in the second brackets between Λ_0 and Λ_1 . A new interaction in $H_{eff}^{\Lambda_1}$ which distinguishes it from H^{Λ_1} arises from the double commutator term in Eq. [22] when it is evaluated for matrix elements satisfying Eq. [19]. $H_{eff}^{\Lambda_1}$ is thus given by

$$H_{eff}^{\Lambda_1} = H_0 + gV_1^{\Lambda_1} + g^2V_2^{\Lambda_1} + g^2V_{self.C}^{\Lambda_1} + g^2V_T^{\Lambda_1} + O(g^3). \quad (24)$$

where

$$\langle m|V_2^{\Lambda_1} + V_{self.C}^{\Lambda_1}|n\rangle = \theta(\Lambda_1 - |E_{mn}|)\langle m|V_2 + V_{self.C}|n\rangle. \quad (25)$$

The last term in Eq. [24] has been generated by the similarity transformation and is meant to reproduce the physics lost when the cutoff is reduced from Λ_0 to Λ_1 . For sharp cutoffs (see Eq. [11]) one has

$$\langle m|V_T^{\Lambda_1}|n\rangle = \theta(\Lambda_1 - |E_{mn}|) \sum_q \langle m|V_1|q\rangle \langle q|V_1|n\rangle \Theta_T(E_{qn}, E_{qm}; \Lambda_1). \quad (26)$$

Note that the sum over intermediate states is cut-off from above due to an implicit dependence of the matrix elements of V_1 on Λ_0 . The last factor is a function which arises in the similarity transformation and is similar to an energy denominator in standard perturbation theory. It is given by

$$\Theta_T(\Delta_a, \Delta_b; \Lambda) = -\frac{\theta(|\Delta_a| - \Lambda)}{\Delta_a} \left(1 - \frac{1}{2}\theta(|\Delta_b| - \Lambda)\right) + (a \leftrightarrow b) \quad (27)$$

Notice, that energy denominators never cause divergences since they are cut off from below by Λ_1 .

We are now in a position to study the ultraviolet behavior of the theory. As Λ_0 approaches infinity $V_2^{\Lambda_1}$ is finite since it is cutoff at the lower scale Λ_1 . Alternatively, the self energy $V_{self.C}$ diverges as $\Lambda_0^C = \Lambda_0 \rightarrow \infty$. Similarly, the effective interaction $V_T^{\Lambda_1}$ contains self energy pieces which diverge and interaction pieces which are ultraviolet finite. Thus it is convenient to split it into two portions

$$V_T^{\Lambda_1} = V_{self.T}^{\Lambda_1} + V_{ex.T}^{\Lambda_1}, \quad (28)$$

where

$$g^2 V_{self,T}^{\Lambda_1} = \sum_{\tau} \int \frac{d\mathbf{k}}{(2\pi)^3} \Sigma_T(\mathbf{k}; \Lambda_0, \Lambda_1) [b^\dagger(\mathbf{k}, \tau) b^\dagger(\mathbf{k}, \tau) + d^\dagger(-\mathbf{k}, \tau) d(-\mathbf{k}, \tau)] \\ + \theta\left(\frac{\Lambda_1}{2} - E(\mathbf{k})\right) G_T(\mathbf{k}; \Lambda_0, \Lambda_1) [b^\dagger(\mathbf{k}, \tau) d^\dagger(-\mathbf{k}, \tau) + d(-\mathbf{k}, \tau) b(\mathbf{k}, \tau)] \quad (29)$$

and $V_{ex,T}$ has a similar structure to V_2 . The functions Σ_T and G_T are given in the Appendix. As stated above, in the limit $\Lambda_0 \rightarrow \infty$, $V_{self,T}^{\Lambda_1}$ is divergent while the exchange interaction, $V_{ex,T}^{\Lambda_1}$ remains finite.

The divergences in the self energy pieces must be absorbed by adding appropriate counter-terms to the bare Hamiltonian. Thus we define

$$H = \lim_{\Lambda_0 \rightarrow \infty} [H^{\Lambda_0} + g^2 V_{ct.}^{\Lambda_0}] \quad (30)$$

Since only one-body operators are explicitly UV divergent we construct counter-terms of the form

$$g^2 V_{ct.}^{\Lambda_0} = \sum_{\tau} \int \frac{d\mathbf{k}}{(2\pi)^3} \Sigma^{ct.}(\mathbf{k}; \Lambda_0) [b^\dagger(\mathbf{k}, \tau) b(\mathbf{k}, \tau) + d^\dagger(-\mathbf{k}, \tau) d(-\mathbf{k}, \tau)] \\ + \theta\left(\frac{\Lambda_0}{2} - E(\mathbf{k})\right) G^{ct.}(\mathbf{k}; \Lambda_0) [b^\dagger(\mathbf{k}, \tau) d^\dagger(-\mathbf{k}, \tau) + d(-\mathbf{k}, \tau) b(\mathbf{k}, \tau)]. \quad (31)$$

Note that $V_{ct.}^{\Lambda_0}$ contains a piece which is off-diagonal in the perturbative basis ($G^{ct.}$). This will lead to a contribution from $V_{ct.}^{\Lambda_0}$ in R_2 when $H^{\Lambda_0} + g^2 V_{ct.}^{\Lambda_0}$ is used as an input to the similarity transformation (as it should be). This extra contribution to R_2 removes couplings caused by $G^{ct.}$ when $\Lambda_1 < 2E(\mathbf{k}) < \Lambda_0$ and therefore only leaves a nonvanishing contribution from this counter-term for $\Lambda_1 > 2E(\mathbf{k})$.

C. The Renormalization Group Improved Hamiltonian

Our goal is to define an effective Hamiltonian which is operative at hadronic scales. Thus one may be tempted to set $\Lambda_1 \sim 1 \text{ fm}^{-1}$. However, a single-step similarity transformation which evolves the Hamiltonian from the UV cut-off Λ_0 down to the hadronic scale would introduce effective interactions with large matrix elements for which the perturbative approach

is hard to justify. This would also result in a large sensitivity of the effective Hamiltonian to parameters which are set at the UV scale. Instead we may use the renormalization transformation iteratively over many small steps and at each step adjust the Hamiltonian only by a small amount. In the language of standard Feynman perturbation theory, the two approaches correspond to keeping only the leading-log and summing the leading-log to all orders, respectively. Thus we choose to apply the similarity transformation

$$N = \frac{\log \frac{\Lambda_0}{\Lambda_N}}{\log(1 + \epsilon)} \quad (32)$$

times starting at the beginning of the renormalization group trajectory with the bare Hamiltonian, $H^{\Lambda_0} = H_{eff}^{\Lambda_0}$ and finishing at the end of the trajectory with $H_{eff}^{\Lambda_N}$. Each time the transformation is applied the cutoff is reduced from Λ_i to Λ_{i+1} by a finite amount

$$\frac{\Lambda_i}{\Lambda_{i+1}} = 1 + \epsilon. \quad (33)$$

The limit $\Lambda_0 \rightarrow \infty$ corresponds to $N\epsilon$ diverging logarithmically.

Expanding the integrands in the expressions for $V_{self,C}$ and $V_{self,T}$ (Eqs. [15] and [29]) in powers of ϵ yields (see Appendix),

$$\begin{aligned} \Sigma_T(\mathbf{k}; \Lambda_0, \Lambda_1) &\rightarrow \epsilon \frac{g^2 C_F}{(4\pi)^2} \left[\frac{2m^2}{E(\mathbf{k})} - \frac{8\mathbf{k}^2}{3E(\mathbf{k})} \right] \left(1 + O\left(\frac{1}{e^{N\epsilon}}\right) \right) \\ \Sigma_C(\mathbf{k}; \Lambda_0) &\rightarrow \epsilon \frac{g^2 C_F}{(4\pi)^2} \left[\frac{4m^2}{E(\mathbf{k})} + \frac{8\mathbf{k}^2}{3E(\mathbf{k})} \right] \left(1 + O\left(\frac{1}{e^{N\epsilon}}\right) \right) + \Sigma_C(\mathbf{k}; \Lambda_1) \\ G_T(\mathbf{k}; \Lambda_0, \Lambda_1) &\rightarrow -\epsilon \frac{g^2 C_F}{(4\pi)^2} \frac{14|\mathbf{k}|m}{3E(\mathbf{k})} \theta\left(\frac{\Lambda_1}{2} - E(\mathbf{k})\right) \left(1 + O\left(\frac{1}{e^{N\epsilon}}\right) \right) \\ G_C(\mathbf{k}; \Lambda_0) &\rightarrow G_C(\mathbf{k}; \Lambda_0, \Lambda_1) \rightarrow -\epsilon \frac{g^2 C_F}{(4\pi)^2} \frac{4|\mathbf{k}|m}{3E(\mathbf{k})} \theta\left(\frac{\Lambda_1}{2} - E(\mathbf{k})\right) \left(1 + O\left(\frac{1}{e^{N\epsilon}}\right) \right) \\ &\quad + G_C(\mathbf{k}; \Lambda_1, \Lambda_1). \end{aligned} \quad (34)$$

The presence of the last terms in the second and fourth equations above causes a complication. Since Λ_N is fixed at the end of the trajectory these terms are of $O(N\epsilon)$ and dominate transverse self energies generated by the similarity transformation, which are of $O(\epsilon)$ (the first and third equations of Eq. [34]). In order for these two types of self energies to be

comparable, most of the Coulomb self energy induced by normal ordering must be subtracted by a counter-term in the original Hamiltonian. An unusual feature of this is that the subtraction must depend on the renormalization group trajectory (as opposed to standard perturbation theory). In other words it is not enough to fix the Coulomb counter-term in H^{Λ_0} , it must also depend on the trajectory (*i.e.*, it must be ϵ -dependent). This is to be expected: covariance relates both Coulomb and transverse gluon exchange and since the similarity transformation affects only the latter, Coulomb self-energies must be adjusted in an appropriate fashion along the entire trajectory.

For a Hamiltonian evaluated at Λ_i along a trajectory defined by Eq. [33] the counter-term is given by

$$\Sigma^{ct.}(\mathbf{k}, \Lambda_i) \rightarrow \Sigma^{ct.}(\mathbf{k}, \Lambda_i; \epsilon) = -\Sigma_C(\mathbf{k}, \frac{\Lambda_i}{1 + \epsilon}) \quad (35)$$

and

$$G^{ct.}(\mathbf{k}, \Lambda_i) \rightarrow G^{ct.}(\mathbf{k}, \Lambda_i, \epsilon) = -G_C(\mathbf{k}; \frac{\Lambda_i}{1 + \epsilon}, \Lambda_{i-1}). \quad (36)$$

The first portion of each equation is meant to indicate that the counter-terms have become trajectory dependent. Possible finite pieces have not been considered in these expressions (*i.e.*, scheme dependence) since they become irrelevant upon use of the renormalization group equations.

At this stage the perturbative portion of the Hamiltonian is fully specified and we are ready to apply the renormalization group procedure. After a single step ($\Lambda_0 \rightarrow \Lambda_1$) a new one-body operator is generated,

$$\begin{aligned} & \int \frac{d\mathbf{k}}{(2\pi)^3} \left[\sqrt{\mathbf{k}^2 + m^2} + \Sigma(\mathbf{k}; \Lambda_0, \epsilon) \right] [b^\dagger(\mathbf{k}, \tau)b(\mathbf{k}, \tau) + d^\dagger(-\mathbf{k}, \tau)d(-\mathbf{k}, \tau)] \\ & + \int \frac{d\mathbf{k}}{(2\pi)^3} \theta\left(\frac{\Lambda_1}{2} - E(\mathbf{k})\right) G(\mathbf{k}; \Lambda_0, \epsilon) [b^\dagger(\mathbf{k}, \tau)d^\dagger(-\mathbf{k}, \tau) + d(-\mathbf{k}, \tau)b(\mathbf{k}, \tau)]. \end{aligned} \quad (37)$$

We have defined new quantities

$$\Sigma(\mathbf{k}; \Lambda_0, \epsilon) = \Sigma_T(\mathbf{k}; \Lambda_0, \Lambda_1) + \Sigma_C(\mathbf{k}, \Lambda_0) + \Sigma^{ct.}(\mathbf{k}, \Lambda_0, \epsilon) = \epsilon \frac{g^2 C_F}{(4\pi)^2} \frac{6m^2}{E(\mathbf{k})} \left(1 + O\left(\frac{1}{e^{N\epsilon}}\right) \right) \quad (38)$$

and

$$G(\mathbf{k}; \Lambda_0, \epsilon) = G_T(\mathbf{k}; \Lambda_0, \Lambda_1) + G_C(\mathbf{k}, \Lambda_0) + G^{ct.}(\mathbf{k}, \Lambda_0, \epsilon) = -\epsilon \frac{g^2 C_F}{(4\pi)^2} \frac{6|\mathbf{k}|m}{E(\mathbf{k})} \left(1 + O\left(\frac{1}{e^{N\epsilon}}\right) \right). \quad (39)$$

The last equality in each equation follows from Eqs. [34], [35], and [36]. In order to iterate the similarity transformation further the one body operator (Eq. [37]) must be diagonalized. This is because the eigenstates of this operator must be used as a new basis in which matrix elements of the interaction are regulated. We therefore proceed by rotating the quarks back to the massless basis ($b, d \rightarrow \hat{b}, \hat{d}$). Eq. [37] then becomes

$$\begin{aligned} & \int \frac{d\mathbf{k}}{(2\pi)^3} \left[|\mathbf{k}| + \mathcal{O}\left(\frac{g^2}{e^{N\epsilon}}\right) \right] [\hat{b}^\dagger(\mathbf{k}, \tau) \hat{b}(\mathbf{k}, \tau) + \hat{d}^\dagger(-\mathbf{k}, \tau) \hat{d}(-\mathbf{k}, \tau)] \\ & - m_1 \int \frac{d\mathbf{k}}{(2\pi)^3} \theta\left(\frac{\Lambda_1}{2} - E(\mathbf{k})\right) [\hat{b}^\dagger(\mathbf{k}, \tau) \hat{d}^\dagger(-\mathbf{k}, \tau) + \hat{d}(-\mathbf{k}, \tau) \hat{b}(\mathbf{k}, \tau)] \end{aligned} \quad (40)$$

where

$$m_1 = m \left[1 + g^2 \frac{6C_F}{(4\pi)^2} \epsilon \left(1 + \mathcal{O}\left(\frac{1}{e^{N\epsilon}}\right) \right) \right] \quad (41)$$

Note that it is only necessary to rotate the basis below the scale Λ_1 so that the θ -functions may be ignored in this process.

To order g^2 this looks just like the free Hamiltonian with m replaced by m_1 and quantized in a massless basis. We now rotate the one body operator back to the massive quark basis using m_1 as the bare quark mass and obtain a free, diagonal Hamiltonian, $H_{eff}^{\Lambda_1}(m_1)$ which may be used as input to the next similarity transformation ($\Lambda_1 \rightarrow \Lambda_2$). Note that since the similarity transformation is only affected to order g^2 by these rotations, the net effect of this procedure is simply to replace $m_0 = m(\Lambda_0)$ by $m_1 = m(\Lambda_1)$. The remainder of the renormalization group procedure is simple: we apply the above transformations N times and obtain an effective Hamiltonian with the one-body operator given by the free Hamiltonian with the replacement $m_0 \rightarrow m_N = m(\Lambda_N)$:

$$m_0 \rightarrow m_N = m \left[1 + g^2 \frac{6C_F}{(4\pi)^2} \epsilon \left(1 + O\left(\frac{1}{e^{N\epsilon}}\right) \right) \right]^N. \quad (42)$$

In the limit $N\epsilon \sim \log \Lambda_0/\Lambda_N \rightarrow \infty$ this becomes

$$m(\Lambda_N) = m(\Lambda_0) \left(\frac{\Lambda_0}{\Lambda_N} \right)^{g^2 \frac{6C_F}{(4\pi)^2}}. \quad (43)$$

Finally, the remainder of the RGI Hamiltonian (the two-body terms) is given by the interactions defined at the end scale

$$gV_1^{\Lambda_N} + g^2V_2^{\Lambda_N} + g^2V_{ex.T}^{\Lambda_N}. \quad (44)$$

It is perhaps useful to summarize the calculation to this point. We have started with the exact Coulomb gauge Hamiltonian of QCD, expanded it to order g^2 , and regulated it in a manner which lends itself to the similarity transformation renormalization procedure. Performing the transformation generated Coulomb and transverse gluon exchange self energy effective interactions which diverge in the ultraviolet limit. The divergences were absorbed into counter-terms and the whole process was iterated to construct the RGI Hamiltonian. This Hamiltonian is defined at a hadronic scale Λ_N , is ultraviolet and infrared finite, and has nonzero matrix elements only for states which differ in energy by up to Λ_N (higher energy physics is incorporated in the effective interaction, $V_{ex.T}$). Notice that all self energy interactions have been absorbed by the renormalization procedure and no longer explicitly appear in the Hamiltonian. As expected for the Coulomb gauge, there is no need for wave function renormalization and the coupling constant does not run until $O(g^3)$.

D. The Phenomenological Interaction

The RGI Hamiltonian which we have constructed can be reliably employed to calculate observables down to a scale of $\Lambda \sim 1\text{fm}^{-1}$ where the coupling constant becomes large (note that we shall refer to the end point of the renormalization group trajectory as Λ from now on). At this point the Hamiltonian must both be solved nonperturbatively and must

be supplemented with a phenomenological potential which incorporates as much of the neglected higher order physics as possible. The latter forms the topic of this section.

Choosing an effective low energy interaction is not trivial because the model is relativistic. This means that a Dirac structure must be imposed on the interaction – with commensurate implications on phenomenology. It is commonly held that the effective potential should be linear with a scalar current interaction. However, we have shown that this simple expectation is misleading [8]. One may establish the Dirac nature of the low energy effective potential in the heavy quark limit. In this case it is appropriate to make a nonrelativistic reduction and use the quenched approximation. P -wave splittings in the J/ψ and Υ spectra imply that long range spin-dependent potentials correspond to a nonrelativistic reduction of a scalar, phenomenological, confining interaction [9]. This view is also supported by lattice gauge calculations [9] and phenomenological, minimal-area-law model for the Wilson loop [11]. Starting with the Coulomb gauge Hamiltonian, it is possible to show that the effective scalar interaction arises dynamically through mixing with hybrids while the static part of the $\bar{q}q$ potential remains of a timelike-vector nature [8].

If one assumes that the heavy quark potential also applies for light quarks then the net result is to simply replace the order g^2 Coulomb potential with a Coulomb plus linear potential:

$$-g^2 C_F \frac{1}{4\pi r} \rightarrow -g^2 C_F \frac{1}{4\pi r} + \sigma r. \quad (45)$$

We shall fix the string tension at $\sigma = 0.18 \text{ GeV}^2$, commensurate with Regge phenomenology, lattice gauge theory, and the constituent quark model. Note that the phenomenological two-body potential is meant to reproduce low energy physics, thus Eq. [45] is used in the effective Hamiltonian, *i.e.*, below the scale Λ . We also introduce a one-body quark operator which corresponds to the linear term in Eq. [45]. This eliminates color non-singlet states from the spectrum. Furthermore, it ensures that color-singlet bound states are infrared-finite.

These observations will be discussed in greater detail below. The final form for the quark sector of the model Hamiltonian which we shall use in subsequent calculations is:

$$H_{DQM} = H_0(\Lambda) + gV_1^\Lambda + g^2V_2^\Lambda + g^2V_{ex,T}^\Lambda + V_{conf} + V_{self.conf}. \quad (46)$$

This has been defined at the scale Λ ; hence the interaction terms are all cutoff at this scale. As discussed above, the Λ dependence of H_0 comes from the running mass. Finally V_{conf} has only two-body matrix elements.

III. EFFECTIVE OPERATORS

If one wishes to make statements about matrix elements which are accurate to order g^2 it is not sufficient to know the states (*i.e.*, the Hamiltonian) to this order – one must also evolve the relevant operator. This is illustrated below with explicit calculations of the perturbative evolution of the single quark operator, the axial charge operator, and the composite operator $\bar{q}q$ used to define the chiral quark condensate.

Just as with the Hamiltonian, one may use the similarity renormalization scheme to calculate effective operators restricted to P -space. Following the steps discussed in Sec. II we first define an operator \mathcal{O}^{Λ_0} by restricting its matrix elements in the basis of eigenstates of H_0 ,

$$\langle m | \mathcal{O} | n \rangle \rightarrow \langle m | \mathcal{O}^{\Lambda_0} | n \rangle = \theta(\Lambda_0 - |E_{mn}|) \langle m | \mathcal{O} | n \rangle \quad (47)$$

The effective operator is then given by

$$\mathcal{O}_{eff} = S \mathcal{O} S^{-1} = \mathcal{O} + ig[R_1, \mathcal{O}] + g^2 \left([R_2, \mathcal{O}] - \frac{1}{2} [R_1, [R_1, \mathcal{O}]] \right) + O(g^3) \quad (48)$$

Notice that in contrast to the evaluation of the Hamiltonian, explicit expressions for R_1 and R_2 are required to compute one-loop corrections to operators. In terms of eigenstates of H_0 these are

$$\langle m | R_1 | n \rangle = i\theta(\Lambda_1 - |E_{mn}|) \frac{\langle m | V_1 | n \rangle}{E_{nm}} \quad (49)$$

and

$$\langle m | R_2 | n \rangle = i \frac{\theta(\Lambda_1 - |E_{nm}|)}{E_{nm}} \left(\langle m | V_2 | n \rangle + \sum_q \langle m | V_1 | q \rangle \langle q | V_1 | n \rangle \Theta_T(E_{qn}, E_{qm}; \Lambda_1) \right). \quad (50)$$

Calculating radiative corrections to operators thus becomes a straightforward, albeit tedious, process of evaluating commutators. Note that the similarity transformation may be iterated to form the renormalization group improved effective operator, just as for the Hamiltonian.

Matrix elements of an operator \mathcal{O} ,

$$\langle m | \mathcal{O} | n \rangle = \langle m | S^{-1} \mathcal{O}_{eff} S | n \rangle \quad (51)$$

have mixings to eigenstates with large energy included perturbatively in \mathcal{O}_{eff} . This enables one to resolve an ambiguity in applying perturbative QCD to hadronic matrix elements. The ambiguity is illustrated in Fig. 1 where two possible diagrams contributing to the hadronic matrix element of a generic current are presented. The question is if the current couples to nonvalence structure in the hadron (say, the strangeness content of the proton), does it do so via an existing nonvalence component of the wave function (as in Fig. 1a) or via a virtual quark loop (as in Fig. 1b)? It is impossible to resolve this in typical approaches to this problem (*i.e.*, without reference to dynamics). The method presented here allows one to identify both contributions. Fig. 1a follows from solving the bound state effective Hamiltonian in a basis which allows the appropriate Fock state mixing. Thus the intermediate states associated with the wave function exist *below* Λ . Alternatively, Fig. 1b arises from transforming the current $\mathcal{O} \rightarrow \mathcal{O}_{eff}$ and involves intermediate states which exist *above* Λ . We emphasize that correctly interpreting this situation can only be done in the context of a consistent dynamical model.

FIGURES



Fig. 1. Resolving Ambiguities in Current Matrix Elements.

A. The Effective Quark Operator

As a first simple application of the similarity transformation we evaluate the one-loop correction to the bare quark operator, $b(\mathbf{k}, \tau)$. This means evaluating the commutators indicated in Eq. [48] with $\mathcal{O} = b(\mathbf{k}, \tau)$. Since we are interested in the evolution of the operator itself (and not the generation of new operators such as ba^\dagger), the first order commutator $[[R_1, b(\mathbf{k}, \tau)]]$ does not contribute. Furthermore the order g^2 commutator, $[R_2, b(\mathbf{k}, \tau)]$, is zero. This is because the first term in R_2 (see Eq. [50]) involves the Coulomb potential which is normal ordered. Thus all commutators with the quark annihilation operator simply yield terms which are proportional to the Coulomb interaction (and never $b(\mathbf{k}, \tau)$). The commutators of the second term in R_2 cancel in pairs and again, do not contribute. Thus the only contribution to b_{eff} is the double commutator over R_1 in Eq. [48]. Two of the 64 possible terms are nonzero, these are shown diagrammatically in Fig. 2a,b. As Fig. 2 indicates, the process of evaluating commutators for \mathcal{O}_{eff} is similar to performing time-ordered perturbation theory. However, we warn the reader that this is an analogy only since nontrivial cut-off dependence is implicit in each diagram.

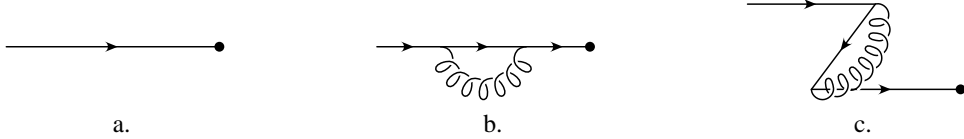


Fig. 2. Diagrams Contributing to b_{eff} .

Expressions for these contributions to b_{eff} are respectively

$$-g^2 \frac{C_F}{4} \int \frac{d\mathbf{p}}{(2\pi)^3} \frac{(1 - \hat{\mathbf{p}} \cdot \hat{\mathbf{l}} \hat{\mathbf{k}} \cdot \hat{\mathbf{l}})}{\omega(\mathbf{l})} \frac{\Theta(\Lambda_0 > |E(\mathbf{p}) + \omega(\mathbf{l}) - E(\mathbf{k})| > \Lambda_1)}{(E(\mathbf{p}) + \omega(\mathbf{l}) - E(\mathbf{k}))^2} \quad (52)$$

$$-g^2 \frac{C_F}{4} \int \frac{d\mathbf{p}}{(2\pi)^3} \frac{(1 + \hat{\mathbf{p}} \cdot \hat{\mathbf{l}} \hat{\mathbf{k}} \cdot \hat{\mathbf{l}})}{\omega(\mathbf{l})} \frac{\Theta(\Lambda_0 > |E(\mathbf{p}) + \omega(\mathbf{l}) + E(\mathbf{k})| > \Lambda_1)}{(E(\mathbf{p}) + \omega(\mathbf{l}) + E(\mathbf{k}))^2}, \quad (53)$$

here we have taken $\mathbf{l} = \mathbf{p} - \mathbf{k}$ and $\Theta(a > b > c) = \theta(b - c)\theta(a - b)$. Applying the similarity transformation $N \sim \log \Lambda_0/\Lambda_N$ times to reduce the cut-off from Λ_0 to Λ_N yields the following leading order result

$$b(\mathbf{k}, \tau) \rightarrow b(\mathbf{k}, \tau) \left(\frac{\Lambda_0}{\Lambda_N} \right)^{-C_F \frac{g^2}{(4\pi)^2}} \quad (54)$$

When the similarity scale equals the ultraviolet cutoff, no renormalization of the quark operator occurs as expected. As the similarity scale is reduced, the “strength” of the quark operator diminishes as “non-diagonal” operators (such as ba^\dagger) become important.

B. The Axial Charge at One-loop

As a simple application of the renormalization of composite operators, we now apply the methodology to the axial charge operator for massless quarks. In terms of bare quark operators this is given as

$$Q_5 = \sum_{\tau} \int \frac{d\mathbf{k}}{(2\pi)^3} \sigma \cdot \hat{k} [b^\dagger(\mathbf{k}, \tau) b(\mathbf{k}, \tau) + d^\dagger(\mathbf{k}, \tau) d(\mathbf{k}, \tau)]. \quad (55)$$

In this case the first six diagrams of Fig. 3 contribute to the perturbative corrections to Q_5 (where now the dot refers to $\mathcal{O} = Q_5$). The Coulomb loop diagrams (Figs. 3.g and h) are zero because Q_5 does not contain terms proportional to $b^\dagger d^\dagger$ or bd . Doing the requisite spin sums and performing the integral over loop momentum and \mathbf{k} leads to the same integrals for Figs. 3.a and 3.b as in Eqs. [52] and [53]. These are cancelled by the vertex correction integral of Fig. 3.c. The same holds for the Z-graphs of Figs. 3.d,e, and f. Thus there is no correction to Q_5 at order g^2 . This is as expected because the axial current is partially conserved and carries no anomalous dimension.

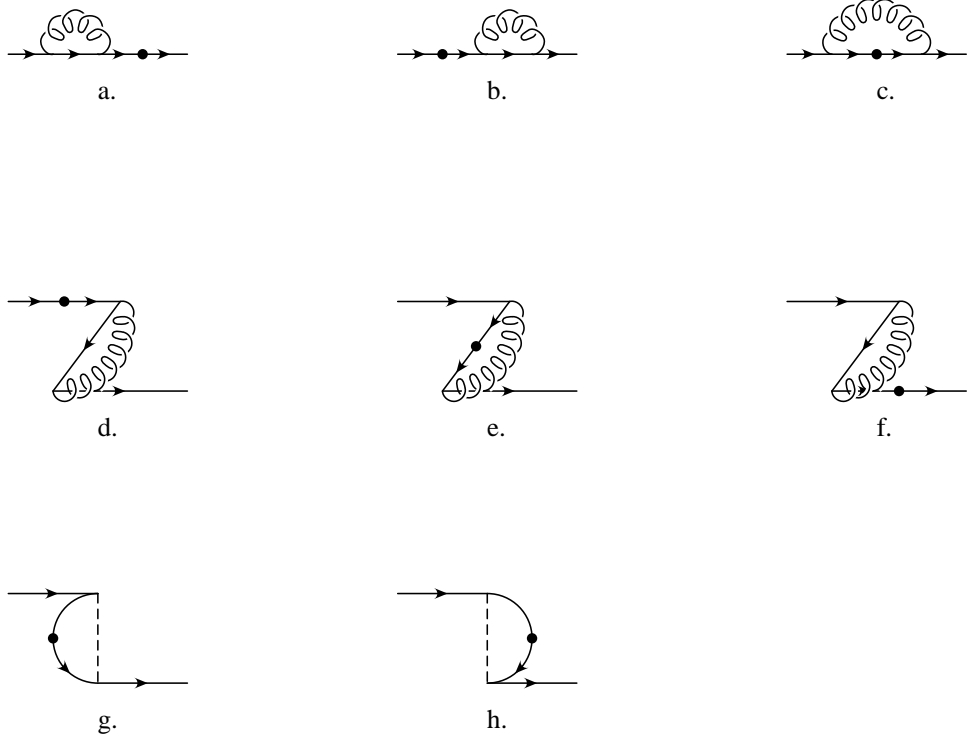


Fig. 3. Diagrams Contributing to \mathcal{O}_{eff} .

C. Renormalization of $\bar{q}q$

The evaluation of Eq. [48] in the case of the $\bar{q}q$ operator is more involved than in the case of the axial charge because diagrams which correspond to $b^\dagger b$ and $d^\dagger d$ also contribute. The regulated operator $\bar{q}q^{\Lambda_0}$ is

$$\begin{aligned} \bar{q}q^{\Lambda_0} = & \sum_{\tau} \int \frac{d\mathbf{q}}{(2\pi)^3} \left[s(\mathbf{q}) [b^\dagger(\mathbf{q}, \tau) b(\mathbf{q}, \tau) + d^\dagger(-\mathbf{q}, \tau) d(-\mathbf{q}, \tau)] \right. \\ & \left. - c(\mathbf{q}) \theta\left(\frac{\Lambda_0}{2} - E(\mathbf{q})\right) [b^\dagger(\mathbf{q}, \tau) d^\dagger(-\mathbf{q}, \tau) + d^\dagger(-\mathbf{q}, \tau) b(\mathbf{q}, \tau)] \right] \\ & - \sum_{\tau} \int \frac{d\mathbf{q}}{(2\pi)^3} s(\mathbf{q}) \end{aligned} \quad (56)$$

where $s(\mathbf{q})$ and $c(\mathbf{q})$ are given by

$$s(\mathbf{q}) = \frac{m_0}{\sqrt{q^2 + m_0^2}} \quad (57)$$

$$c(\mathbf{q}) = \frac{|\mathbf{q}|}{\sqrt{q^2 + m_0^2}}. \quad (58)$$

After similarity transformation the effective operator $\bar{q}q_{eff}^{\Lambda_1}$ can be written as

$$\begin{aligned}\bar{q}q^{\Lambda_0} = & \bar{q}q^{\Lambda_1} + g^2 \frac{C_F}{(4\pi)^2} \sum_{\tau} \int \frac{d\mathbf{k}}{(2\pi)^3} \left[-A_s(\mathbf{k}; \Lambda_0, \Lambda_1) [b^\dagger(\mathbf{k}, \tau)b(\mathbf{k}, \tau) + d^\dagger(-\mathbf{k}, \tau)d(-\mathbf{k}, \tau)] \right. \\ & \left. - A_c(\mathbf{k}; \Lambda_0, \Lambda_1) [b^\dagger(\mathbf{k}, \tau)d^\dagger(-\mathbf{k}, \tau) + d(-\mathbf{k}, \tau)b(\mathbf{k}, \tau)] \right]\end{aligned}\quad (59)$$

Recall that $\bar{q}q^{\Lambda_0} = \bar{q}q_{eff}^{\Lambda_1}$ by definition. The integrands in this expression may be separated into portions representing contributions from $[R_2, \bar{q}q]$ and $[R_1, [R_1, \bar{q}q]]$ respectively:

$$A_s = A_{s2} + A_{s11}, \quad A_c = A_{c2} + A_{c11}. \quad (60)$$

The commutator $[R_1, \bar{q}q^{\Lambda_0}]$ leads to an effective operator that changes the number of gluons by ± 1 and hence need not be considered. The parts of these commutators which give rise to the leading renormalization group trajectory are given by

$$\begin{aligned}A_{s2}(\mathbf{k}; \Lambda_0, \Lambda_1) = & s(\mathbf{k}) \log \frac{\Lambda_0}{2} \left[8 - 4\theta(|\mathbf{k}| + E(\mathbf{k}) - \Lambda_1) \left(1 - \frac{\Lambda_1 - E(\mathbf{k})}{|\mathbf{k}|} \right) \right] \\ & + s(\mathbf{k}) \int d|\mathbf{q}| d(\hat{\mathbf{q}} \cdot \hat{\mathbf{k}}) \theta\left(\frac{\Lambda_0}{2} - |\mathbf{q}|\right) \left[\frac{\theta(\Lambda_0 > |E(\mathbf{k}) - E(\mathbf{q}) + \omega(\mathbf{k} - \mathbf{q})| > \Lambda_1)}{-E(\mathbf{k}) - E(\mathbf{q}) + \omega(\mathbf{k} - \mathbf{q})} \right. \\ & \left. + \frac{\theta(\Lambda_0 > |E(\mathbf{k}) - E(\mathbf{q}) + \omega(\mathbf{k} - \mathbf{q})| > \Lambda_1)}{E(\mathbf{k}) - E(\mathbf{q}) + \omega(\mathbf{k} - \mathbf{q})} \right].\end{aligned}\quad (61)$$

and

$$\begin{aligned}A_{c2}(\mathbf{k}; \Lambda_0, \Lambda_1) = & c(\mathbf{k}) \log \frac{\Lambda_0}{2} \left[8 - 4\theta(|\mathbf{k}| + E(\mathbf{k}) - \Lambda_1) \left(1 - \frac{\Lambda_1 - E(\mathbf{k})}{|\mathbf{k}|} \right) \right] \\ & + \int d|\mathbf{q}| d(\hat{\mathbf{q}} \cdot \hat{\mathbf{k}}) \theta\left(\frac{\Lambda_0}{2} - |\mathbf{q}|\right) \left[(c(\mathbf{k}) + \hat{\mathbf{k}} \cdot \hat{\mathbf{q}}) \frac{\theta(\Lambda_0 > |E(\mathbf{k}) - E(\mathbf{q}) + \omega(\mathbf{k} - \mathbf{q})| > \Lambda_1)}{-E(\mathbf{k}) - E(\mathbf{q}) + \omega(\mathbf{k} - \mathbf{q})} \right. \\ & \left. + (c(\mathbf{k}) - \hat{\mathbf{k}} \cdot \hat{\mathbf{q}}) \frac{\theta(\Lambda_0 > |E(\mathbf{k}) - E(\mathbf{q}) + \omega(\mathbf{k} - \mathbf{q})| > \Lambda_1)}{E(\mathbf{k}) - E(\mathbf{q}) + \omega(\mathbf{k} - \mathbf{q})} \right].\end{aligned}\quad (62)$$

The remaining terms are

$$A_{s11}(\mathbf{k}; \Lambda_0, \Lambda_1) = -2s(\mathbf{k}) \log \frac{\Lambda_0}{2} - s(\mathbf{k}) \int d|\mathbf{q}| d(\hat{\mathbf{q}} \cdot \hat{\mathbf{k}}) [\dots] \quad (63)$$

and

$$A_{c11}(\mathbf{k}; \Lambda_0, \Lambda_1) = -2c(\mathbf{k}) \log \frac{\Lambda_0}{2} - \int d|\mathbf{q}| d(\hat{\mathbf{q}} \cdot \hat{\mathbf{k}}) [\dots]. \quad (64)$$

The two integrands in A_{s11} and A_{c11} abbreviated by [...] are identical with the integrands in A_{s2} and A_{c2} respectively and therefore cancel in A_s and A_c . The contributions to A_{s2} and A_{c2} which are proportional to $\theta(|\mathbf{k}| + E(\mathbf{k}) - \Lambda_1)$ vanish when matrix elements of $\bar{q}q_{eff}^\Lambda$ are taken in a basis in which $H_{eff}^{\Lambda_1}$ is nonzero *i.e.*, for $\Lambda_1 > 2E(\mathbf{k})$ (see Eq. [19]). The additional contribution to R_2 resulting from off-diagonal self energies (G_C , G_T), discussed below Eq. [31], results in terms proportional to $\theta(2E(\mathbf{k}) - \Lambda_1)$ and also vanishes below the cut-off. Finally, after a single application of the similarity transformation,

$$\bar{q}q^{\Lambda_0} = \left[1 + g^2 \frac{6C_F}{(4\pi)^2} \log \frac{\Lambda_0}{\Lambda_1} \right] \bar{q}q_1^\Lambda + \text{“finite”} = \left[1 + g^2 \frac{6C_F}{(4\pi)^2} \epsilon \left(1 + O\left(\frac{1}{e^{N\epsilon}}\right) \right) \right] \bar{q}q^{\Lambda_1}. \quad (65)$$

The term “finite” refers to contributions which are finite in the limit $\Lambda_0 \rightarrow \infty$, with fixed Λ_1 , and thus do not contribute to the leading renormalization group trajectory. Applying the similarity transformation $N \sim \log \Lambda_0 / \Lambda_N$ times yields,

$$\bar{q}q^{\Lambda_0} = \left(\frac{\Lambda_0}{\Lambda_N} \right)^{6C_F \frac{g^2}{(4\pi)^2}} \bar{q}q^{\Lambda_N}. \quad (66)$$

Using Eq. [43] we may easily show that the product $m\bar{q}q$, is constant along the renormalization group trajectory *i.e.*, as $\Lambda_0 \rightarrow \Lambda_N$

$$m(\Lambda_0)\bar{q}q^{\Lambda_0} = m(\Lambda_N)\bar{q}q^{\Lambda_N}. \quad (67)$$

IV. NONPERTURBATIVE PROPERTIES

It is known that constituent quarks are the appropriate degrees of freedom for the description of hadrons. Since the DQM is constructed with current quarks, constituent quarks must be dynamically generated as the pseudoparticles of the model. We therefore choose to proceed by making a pairing ansatz for the vacuum of the standard BCS form. This is motivated by the constituent quark model as we shall see shortly. The incorporation of a nontrivial pairing vacuum may be easily achieved by performing a Bogoliubov-Valatin canonical transformation on the quark fields:

$$\begin{aligned} B(\mathbf{k}, \tau) &= \cos\left(\frac{1}{2}\phi(\mathbf{k})\right)b(\mathbf{k}, \tau) - h(\tau)\sin\left(\frac{1}{2}\phi(\mathbf{k})\right)d^\dagger(\mathbf{k}, \tau) \\ D(\mathbf{k}, \tau) &= \cos\left(\frac{1}{2}\phi(\mathbf{k})\right)d(\mathbf{k}, \tau) + h(\tau)\sin\left(\frac{1}{2}\phi(\mathbf{k})\right)b^\dagger(\mathbf{k}, \tau) \end{aligned} \quad (68)$$

where $h(\tau) = \pm 1$ is the helicity. The transformation is parameterized in terms of the Bogoliubov angle, $\phi(\mathbf{k})$. In future we shall use the notation

$$S_{\frac{1}{2}}(\mathbf{k}) = \sin\left(\frac{1}{2}\phi(\mathbf{k})\right), \quad S(\mathbf{k}) = \sin(\phi(\mathbf{k})), \quad (69)$$

with similar expressions for the cosine.

Expressing the effective Hamiltonian, H_{eff}^Λ in terms of the constituent quark and antiquark operators (B and D respectively) leads to a one-body off-diagonal operator of the type

$$\sum_\tau \int \frac{d\mathbf{k}}{(2\pi)^3} F(\mathbf{k}; \phi) \left[B^\dagger(\mathbf{k}, \tau) D^\dagger(-\mathbf{k}, \tau) + D(-\mathbf{k}, \tau) B(\mathbf{k}, \tau) \right]. \quad (70)$$

The Bogoliubov angle is chosen so that this operator vanishes

$$F(\mathbf{k}, \phi) = 0; \quad (71)$$

this is the vacuum gap equation of the DQM.

Although the gap equation allows the determination of a nontrivial vacuum, and hence of the dynamical quark mass (discussed below), there is actually another important reason for imposing this structure on the model. In particular, the successes of the constituent quark model indicate that valence quarks saturate hadronic states to a large degree. The BCS ansatz is one of the simplest methods which allows for dynamical chiral symmetry breaking and decoupling of $\bar{q}q$ pairs from the vacuum. Thus the nonperturbative approach we have taken is firmly based on the successes of the CQM. We note that the decoupling of the vacuum does not persist as states with four or more constituents are included in the analysis. In this case it is only possible to approximately diagonalize the Hamiltonian by further changing the basis as it is done, for example in the Random Phase Approximation (RPA) or by using bound state perturbation theory with either Tamm-Dancoff or RPA eigenstates as a basis.

The explicit form of the gap equation is given by:

$$\begin{aligned} & \left[\sqrt{\mathbf{k}^2 + m(\Lambda)^2} + \Sigma_l(\mathbf{k}, \Lambda) \right] S(\mathbf{k}) + \theta\left(\frac{\Lambda}{2} - E(\mathbf{k})\right) G_l(\mathbf{k}; \Lambda) C(\mathbf{k}) = \\ & = \int \frac{d\mathbf{q}}{(2\pi)^3} \left[\left(\mathcal{V}_{cl}^{(1)}(\mathbf{k}, \mathbf{q}) + \mathcal{V}_T^{(1)}(\mathbf{k}, \mathbf{q}) \right) 2S(\mathbf{k}) S_{\frac{1}{2}}^2(\mathbf{q}) + \left(\mathcal{V}_{cl}^{(2)}(\mathbf{k}, \mathbf{q}) + \mathcal{V}_T^{(2)}(\mathbf{k}, \mathbf{q}) \right) C(\mathbf{k}) S(\mathbf{q}) \right. \\ & \left. + \left(\mathcal{V}_{cl}^{(3)}(\mathbf{k}, \mathbf{q}) + \mathcal{V}_T^{(3)}(\mathbf{k}, \mathbf{q}) \right) S(\mathbf{k}) S(\mathbf{q}) + \left(\mathcal{V}_{cl}^{(4)}(\mathbf{k}, \mathbf{q}) + \mathcal{V}_T^{(4)}(\mathbf{k}, \mathbf{q}) \right) 2C(\mathbf{k}) S_{\frac{1}{2}}^2(\mathbf{q}) \right]. \end{aligned} \quad (72)$$

Here the functions $\mathcal{V}_{cl}^{(i)}$ and $\mathcal{V}_T^{(i)}$ come from the static, two-body, Coulomb and linear (denoted by the subscript cl) part of the effective Hamiltonian and the effective interactions resulting from transverse gluon exchange (denoted by T) respectively. They are all summarized in the Appendix. The only self-energy type contributions, Σ_l and G_l , come from the linear potential. As discussed in Sec. IID, these are necessary to maintain the IR stability of physical observables. The importance of the linear self energy term has been noted previously in Refs. [4,12,13]. It should be noted that the solution to the gap equation depends on the scale Λ , $\phi = \phi(\mathbf{k}; \Lambda)$.

Since the gap equation incorporates all order g^2 physics correctly it is completely UV finite. This is not true for earlier work. For example, the gap equation of Le Yaouanc *et al.* [14] may be obtained from this one by setting all theta functions equal to unity and by ignoring all transverse gluon terms. This introduces an ultraviolet divergence due to the Coulomb self-energy term which they avoid by simply neglecting the Coulomb interaction. Adler and Davis [12] discuss the gap equation with a pure Coulomb interaction. It should be noted, however, that in absence of transverse gluons, pure Coulomb exchange leads to momentum dependent counter-terms. Finally, the gap equation of Finger and Mandula [15] is similar to those above except that they ignore all self energy terms. This eliminates all UV divergences but introduces IR divergences. We stress that the only consistent way to derive a gap equation which incorporates gluons is with a well-defined Hamiltonian-based renormalization scheme, such as is presented here.

As $|\mathbf{k}| \rightarrow \infty$ the solution to the gap equation approaches the perturbative result: $S(\mathbf{k}) \rightarrow s(\mathbf{k})$. It is thus natural to define an effective quark mass with the relationship

$$s(\mathbf{k}; m_{dyn}(\mathbf{k})) = S(\mathbf{k}). \quad (73)$$

The dispersion relation for such a dynamical quark mass is shown in Fig. 4 (the bare quark mass was chosen to satisfy $m(1 \text{ GeV}) = 5 \text{ MeV}$). The solid line is $E(k; \Lambda)$ for $\Lambda = 4 \text{ GeV}$. The dashed line represents $\sqrt{k^2 + m^2(4\text{GeV})}$ (where the quark mass has been perturbatively run from 1 GeV to 4 GeV). One sees that the correct high energy behavior is recovered and that a constituent quark mass of roughly 100 MeV is obtained at low energy. This is approximately one half of the constituent masses used in relativistic quark models. In general the constituent quark mass will tend to zero as the scale is reduced and will saturate as the scale is increased. A detailed study of the dynamical quark mass is beyond the scope of this paper and will be presented elsewhere.

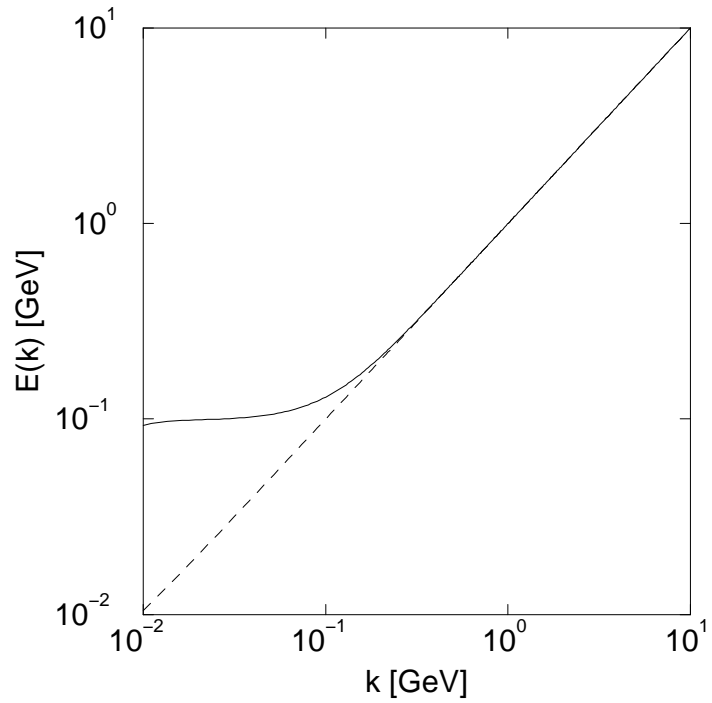


Fig. 4. The Dynamical Quark Dispersion Relation

With a nontrivial solution to the gap equation we may proceed to define the nonperturbative quark condensate. The matrix element of $\bar{q}q_{eff}^\Lambda$ in the nonperturbative vacuum, $|\Omega\rangle$ (defined by $B|\Omega\rangle = D|\Omega\rangle = 0$) is given by (per quark flavor)

$$\langle\Omega|\bar{q}q^\Lambda|\Omega\rangle = -6 \int \frac{d\mathbf{k}}{(2\pi)^3} [S(\mathbf{k})c(\mathbf{k}) + (C(\mathbf{k}) - 1)s(\mathbf{k})]. \quad (74)$$

This expression has been regulated by subtracting the perturbative contribution:

$$\langle 0 | \bar{q}q | 0 \rangle = -6 \int \frac{d\mathbf{k}}{(2\pi)^3} s(k). \quad (75)$$

The condensate is shown as a function of the renormalization scale in Fig. 5. The circles represent the solution for massless quarks while the diamonds are for $m(1\text{GeV}) = 5 \text{ MeV}$. The perturbative solution is shown as a solid line (this has been normalized to match the nonperturbative results). As expected, both nonperturbative curves approach the perturbative solution as Λ increases. The behavior of the condensate below 3 GeV is driven by the nonperturbative renormalization group trajectory of the model. How closely this follows the actual nonperturbative evolution of QCD is a function of how good our approximations are (in particular the form of V_{conf} and the vacuum Ansatz). A way to test the consistency of the model is to calculate the nonperturbative running quark mass and strong coupling constant (and wave function normalization). This may be done, *e.g.*, by fixing Λ (below 3 GeV), calculating several observable (such as the pion and rho masses) and fixing the parameters of the model to reproduce experiment,

$$m_{\pi/\rho}(m(\Lambda), \alpha_S(\Lambda); \Lambda) = m_{\pi/\rho}|_{\text{expt}}. \quad (76)$$

Once the nonperturbative running mass is determined one may compare it to the expected running mass (taking advantage of the renormalization group invariance of $m q\bar{q}$ and the results of Fig. 5.) to assess the accuracy of the model.

The value of the condensate at low energy is roughly $(-100 \text{ MeV})^3$. This does not compare well with the commonly quoted value of $(-250 \text{ MeV})^3$ [1]. The underestimate for both the constituent quark mass and the condensate is most likely due to an inadequate model for the vacuum. More quark correlations may need to be incorporated or a coupled quark-gluon vacuum Ansatz may be required. Unfortunately the use of nonperturbative methods implies that the problem is not restricted to the vacuum sector. For example, the Thouless theorem relates the pairing vacuum to the RPA pion via the Gell-Mann–Oakes–Renner relationship $f_\pi^2 m_\pi^2 = -2m_q \langle q\bar{q} \rangle$ [4]. Thus, if the pion mass is fixed, a poor model of

the vacuum will be reflected in a low value of the pion decay constant. How severe these problems are will be examined in future work. For now, we must remain satisfied that nonperturbative statements about the vacuum can be made at all.

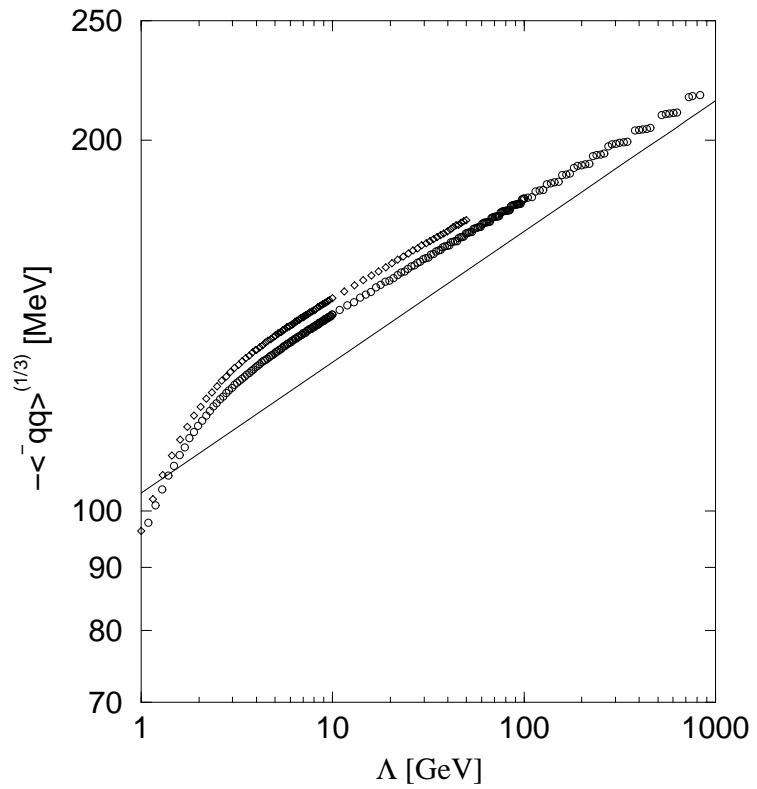


Fig. 5. The Quark Condensate.

V. CONCLUSIONS

This paper presents the development of the Dynamical Quark Model. The model is meant to describe hadronic physics and is therefore designed to be amenable to many-body techniques from the outset. The use of field theoretic methods forces one to choose appropriate degrees of freedom and many-body approximations. The constituent quark model has been used as a guide in this process. For example, the choice of the Coulomb gauge, the form of the gap equation, and the use of the Tamm-Dancoff approximation are all suggested by the phenomenological success of the CQM.

There are three main stages in the construction of the DQM. The first is the evaluation of the renormalization group improved QCD Hamiltonian to order g^2 . This is achieved with a Hamiltonian-based renormalization scheme introduced by G $\ddot{\text{a}}$ z e z and Wilson (the similarity scheme). In the second stage, the RGI Hamiltonian is supplemented with a phenomenological potential. The fact that the starting point of the DQM is QCD provided some important constraints. In particular, the Dirac structure of the phenomenological potential is determined in the heavy quark limit. Performing the Bogoliubov-Valatin transformation comprised the last stage of this program. This allows the construction of a nontrivial vacuum – a necessary feature of the model since constituent quarks must be dynamically generated. A beneficial corollary is the appearance of chiral pions.

Since this paper is meant to describe the perturbative development of the model, only the simplest preliminary applications have been discussed. Thus we have derived and solved the vacuum gap equation, used the resulting Bogoliubov angle to determine the dynamical quark mass, and evaluated the chiral quark condensate. It is satisfying and nontrivial that a constituent quark mass arises and is roughly as expected from phenomenological considerations. This is an indication that the approach we are taking may be useful for light quarks (the DQM may be trusted for heavy quarks since it reduces to the CQM in this case). Unfortunately, the chiral condensate and the constituent quark mass are too small – evidence that the nonperturbative structure of QCD is not fully captured in our model

and approximations. Whether this is a serious problem or not can only be determined by a comparison with more observables. The application (and possible modification) of the DQM to hadronic observables is clearly an important task for the future.

The DQM has a rich structure and therefore allows the examination of many topical issues in hadronic physics. There are several qualitative aspects of the model which we hope to explore in the near future. These include an extension of the phenomenological potential to incorporate nonperturbative gluonic flux tube degrees of freedom and an analysis of hadronic decays in a spirit similar to our discussion of the dynamical generation of effective scalar spin-dependent interactions [8]. It will also be interesting to examine hyperfine splittings in the $N\Delta$ and $\pi\rho$ systems as a function of quark mass. This should shed some light on the genesis and utility of the constituent quark model.

Finally, there is a wealth of specific phenomenological problems in hadronic physics which the DQM may address. For example, since gluonic degrees of freedom are explicitly included in the model, we may examine the properties of glueballs and hybrids – including their couplings to quarkonia. Pions are ubiquitous in hadronic physics, appearing as strongly interacting probes, decay products, and exchange currents. It is therefore essential that they be thoroughly understood. However the chiral and relativistic nature of pions have made this a longstanding deficiency of microscopic models of QCD. It will therefore be interesting to examine a selection of problems which involve pions (recall that pions are relativistic pseudo-Goldstone bosons built from quark pseudoparticles in the DQM). In particular we plan to calculate the pion mass, decay constant, electromagnetic form factor, and the width for $\pi_0 \rightarrow \gamma\gamma$. Many other problems may be addressed with the DQM. We regard the scheme presented here as the next step in a process where models are used to elucidate and guide experiment which in turn directs the development of newer and more sophisticated models of low energy QCD.

ACKNOWLEDGMENTS

Financial support from the U.S. Department of Energy grants No. DE-FG05-88ER40461, DE-FG05-90ER40589, DE-FG02-96ER40944 and Cray time from the North Carolina Supercomputer Center is acknowledged. ES also acknowledges the financial support of an FRPD grant from NCSU.

APPENDIX A:

The functions Σ_C and G_C appearing in Eq. [15] are given by

$$\Sigma_C(\mathbf{k}; \Lambda_0^C) = g^2 C_F \int \frac{d\mathbf{q}}{(2\pi)^3} \theta(\Lambda_0^C - E(\mathbf{q})) \left(s(\mathbf{k})s(\mathbf{q}) + \hat{\mathbf{k}} \cdot \hat{\mathbf{q}} c(\mathbf{k})c(\mathbf{q}) \right) V_c(\mathbf{k}, \mathbf{q}) \quad (A1)$$

$$G_C(\mathbf{k}; \Lambda_0^C) = -g^2 C_F \int \frac{d\mathbf{q}}{(2\pi)^3} \theta(\Lambda_0^C - E(\mathbf{q})) \left(c(\mathbf{k})s(\mathbf{q}) - \hat{\mathbf{k}} \cdot \hat{\mathbf{q}} s(\mathbf{k})c(\mathbf{q}) \right) V_c(\mathbf{k}, \mathbf{q}) \quad (A2)$$

where

$$V_c(\mathbf{k}, \mathbf{q}) = \frac{1}{2|\mathbf{k} - \mathbf{q}|^2}. \quad (A3)$$

The self energies due to transverse gluon exchange are given by

$$\begin{aligned} \Sigma_T(\mathbf{k}; \Lambda_0, \Lambda_1) &= -g^2 C_F \int \frac{d\mathbf{q}}{(2\pi)^3} \left(1 - s(\mathbf{k})s(\mathbf{q}) - \hat{\mathbf{k}} \cdot \hat{\mathbf{l}} \hat{\mathbf{q}} \cdot \hat{\mathbf{l}} c(\mathbf{k})c(\mathbf{q}) \right) \\ &\times \frac{\theta(\Lambda_0 > |E(\mathbf{k}) - E(\mathbf{q}) - \omega(\mathbf{l})| > \Lambda_1)}{2\omega(\mathbf{l}) (\omega(\mathbf{l}) + E(\mathbf{q}) - E(\mathbf{k}))} + \left(-1 - s(\mathbf{k})s(\mathbf{q}) - \hat{\mathbf{k}} \cdot \hat{\mathbf{l}} \hat{\mathbf{q}} \cdot \hat{\mathbf{l}} c(\mathbf{k})c(\mathbf{q}) \right) \\ &\times \frac{\theta(\Lambda_0 > |E(\mathbf{k}) + E(\mathbf{q}) + \omega(\mathbf{l})| > \Lambda_1)}{2\omega(\mathbf{l}) (\omega(\mathbf{l}) + E(\mathbf{q}) + E(\mathbf{k}))} \end{aligned} \quad (A4)$$

and

$$\begin{aligned} G_T(\mathbf{k}; \Lambda_0, \Lambda_1) &= g^2 C_F \int \frac{d\mathbf{q}}{(2\pi)^3} \frac{1}{\omega(\mathbf{l})} \theta(\Lambda_0 - |E(\mathbf{q}) + E(\mathbf{k}) + \omega(\mathbf{l})|) \theta(\Lambda_0 - |E(\mathbf{q}) - E(\mathbf{k}) + \omega(\mathbf{l})|) \\ &\times \left(c(\mathbf{k})s(\mathbf{q}) - \hat{\mathbf{k}} \cdot \hat{\mathbf{l}} \hat{\mathbf{q}} \cdot \hat{\mathbf{l}} c(\mathbf{q})s(\mathbf{k}) \right) \Theta_T(E(\mathbf{q}) + E(\mathbf{k}) + \omega(\mathbf{l}), E(\mathbf{q}) - E(\mathbf{k}) + \omega(\mathbf{l}); \Lambda_1). \end{aligned} \quad (A5)$$

The self energies due to the linear potential appearing in Eq. [72], Σ_l and G_l , are obtained from Σ_c and G_c respectively by substitution

$$g^2 C_F V_c(\mathbf{k}, \mathbf{q}) \rightarrow V_l(\mathbf{k}, \mathbf{q}) = \frac{4\pi\sigma}{|\mathbf{k} - \mathbf{q}|^4}, \quad (\text{A6})$$

where $\sigma = 0.18$ GeV² is the string tension.

The functions $\mathcal{V}_{cl}^{(i)}$ which appear in Eq. [72] are given by

$$\begin{aligned} \mathcal{V}_{cl}^{(1)}(\mathbf{k}, \mathbf{q}) &= \left(s(\mathbf{k})s(\mathbf{q}) + \hat{\mathbf{k}} \cdot \hat{\mathbf{q}} c(\mathbf{k})s(\mathbf{q}) \right) V_{cl}(\mathbf{k}, \mathbf{q}) \\ \mathcal{V}_{cl}^{(2)}(\mathbf{k}, \mathbf{q}) &= \frac{1}{2} \left(c(\mathbf{k})c(\mathbf{q}) + \hat{\mathbf{k}} \cdot \hat{\mathbf{q}} (1 + s(\mathbf{k})s(\mathbf{q})) \right) \Theta_-(\mathbf{k}, \mathbf{q}; \Lambda) V_{cl}(\mathbf{k}, \mathbf{q}) \\ &\quad + \frac{1}{2} \left(c(\mathbf{k})c(\mathbf{q}) - \hat{\mathbf{k}} \cdot \hat{\mathbf{q}} (1 - s(\mathbf{k})s(\mathbf{q})) \right) \Theta_+(\mathbf{k}, \mathbf{q}; \Lambda) V_{cl}(\mathbf{k}, \mathbf{q}) \\ \mathcal{V}_{cl}^{(3)}(\mathbf{k}, \mathbf{q}) &= \left(-s(\mathbf{k})c(\mathbf{q}) + \hat{\mathbf{k}} \cdot \hat{\mathbf{q}} s(\mathbf{q})c(\mathbf{k}) \right) \Theta_{\mathbf{q}}(\mathbf{q}; \Lambda) V_{cl}(\mathbf{k}, \mathbf{q}) \\ \mathcal{V}_{cl}^{(4)}(\mathbf{k}, \mathbf{q}) &= \mathcal{V}_{cl}^{(3)}(\mathbf{q}, \mathbf{k}) \end{aligned} \quad (\text{A7})$$

and

$$\begin{aligned} \mathcal{V}_T^{(1)}(\mathbf{k}, \mathbf{q}) &= \frac{1}{4\omega(\mathbf{l})} \left[1 - s(\mathbf{k})s(\mathbf{q}) - \hat{\mathbf{k}} \cdot \hat{\mathbf{l}} \hat{\mathbf{q}} \cdot \hat{\mathbf{l}} c(\mathbf{k})c(\mathbf{q}) \right] \\ &\quad \times [\Theta_T(E(\mathbf{q}) - E(\mathbf{k}) + \omega(\mathbf{l}), E(\mathbf{q}) - E(\mathbf{k}) + \omega(\mathbf{l}); \Lambda) \\ &\quad + \Theta_T(-E(\mathbf{q}) + E(\mathbf{k}) + \omega(\mathbf{l}), -E(\mathbf{q}) + E(\mathbf{k}) + \omega(\mathbf{l}); \Lambda)] \\ &\quad - \frac{1}{4\omega(\mathbf{l})} \left[1 + s(\mathbf{k})s(\mathbf{q}) + \hat{\mathbf{k}} \cdot \hat{\mathbf{l}} \hat{\mathbf{q}} \cdot \hat{\mathbf{l}} c(\mathbf{k})c(\mathbf{q}) \right] \\ &\quad \times [\Theta_T(-E(\mathbf{q}) - E(\mathbf{k}) + \omega(\mathbf{l}), -E(\mathbf{q}) - E(\mathbf{k}) + \omega(\mathbf{l}); \Lambda) \\ &\quad + \Theta_T(E(\mathbf{q}) + E(\mathbf{k}) + \omega(\mathbf{l}), E(\mathbf{q}) + E(\mathbf{k}) + \omega(\mathbf{l}); \Lambda)] \end{aligned} \quad (\text{A8})$$

$$\begin{aligned} \mathcal{V}_T^{(2)}(\mathbf{k}, \mathbf{q}) &= -\frac{1}{2\omega(\mathbf{l})} \left[c(\mathbf{k})c(\mathbf{q}) - \hat{\mathbf{k}} \cdot \hat{\mathbf{l}} \hat{\mathbf{q}} \cdot \hat{\mathbf{l}} (1 - s(\mathbf{k})s(\mathbf{q})) \right] \Theta_-(\mathbf{k}, \mathbf{q}; \Lambda) \\ &\quad \times \Theta_T(-E(\mathbf{q}) + E(\mathbf{k}) + \omega(\mathbf{l}), E(\mathbf{q}) - E(\mathbf{k}) + \omega(\mathbf{l}); \Lambda) \\ &\quad - \left[c(\mathbf{k})c(\mathbf{q}) + \hat{\mathbf{k}} \cdot \hat{\mathbf{l}} \hat{\mathbf{q}} \cdot \hat{\mathbf{l}} (1 + s(\mathbf{k})s(\mathbf{q})) \right] \Theta_+(\mathbf{k}, \mathbf{q}; \Lambda) \\ &\quad \times \Theta_T(E(\mathbf{q}) + E(\mathbf{k}) + \omega(\mathbf{l}), -E(\mathbf{q}) - E(\mathbf{k}) + \omega(\mathbf{l}); \Lambda) \end{aligned}$$

$$\begin{aligned}
\mathcal{V}_T^{(3)}(\mathbf{k}, \mathbf{q}) &= \frac{1}{2\omega(\mathbf{l})} \left[s(\mathbf{k})c(\mathbf{q}) - \hat{\mathbf{k}} \cdot \hat{\mathbf{l}} \hat{\mathbf{q}} \cdot \hat{\mathbf{l}} c(\mathbf{k})s(\mathbf{q}) \right] \Theta_{\mathbf{q}}(\mathbf{q}, \Lambda) \\
&\times [-\Theta_T(-E(\mathbf{q}) - E(\mathbf{k}) + \omega(\mathbf{l}), E(\mathbf{q}) - E(\mathbf{k}) + \omega(\mathbf{l}); \Lambda) \\
&+ \Theta_T(E(\mathbf{q}) + E(\mathbf{k}) + \omega(\mathbf{l}), -E(\mathbf{q}) + E(\mathbf{k}) + \omega(\mathbf{l}); \Lambda)] \\
\mathcal{V}_T^{(4)}(\mathbf{k}, \mathbf{q}) &= \mathcal{V}_T^{(3)}(\mathbf{q}, \mathbf{k})
\end{aligned} \tag{A9}$$

where V_{cl} is the sum of Coulomb and linear potentials

$$V_{cl}(\mathbf{k}, \mathbf{q}) = \frac{C_F g^2}{2|\mathbf{k} - \mathbf{q}|^2} + \frac{4\pi\sigma}{|\mathbf{k} - \mathbf{q}|^4} \tag{A10}$$

and the effective transverse gluon cut-off Θ_T is given by Eq. [27]. Additional cut-offs are given by

$$\Theta_{\pm}(\mathbf{k}, \mathbf{q}; \Lambda) = \theta(\Lambda - 2|E(\mathbf{k}) \pm E(\mathbf{q})|) \tag{A11}$$

and

$$\Theta_{\mathbf{p}} = \theta(\Lambda - 2E(\mathbf{p})). \tag{A12}$$

Furthermore $s(\mathbf{k})$ and $c(\mathbf{k})$ stand for the sine and cosine of the free particle BV angle *i.e.*,

$$s(\mathbf{p}) = \sin(\phi_m(\mathbf{p})) = \frac{m}{\sqrt{\mathbf{p}^2 + m^2}}, \quad c(\mathbf{p}) = \cos(\phi_m(\mathbf{p})) = \frac{1}{\sqrt{\mathbf{p}^2 + m^2}}. \tag{A13}$$

Finally, $\mathbf{l} = \mathbf{k} - \mathbf{q}$ and $\omega(\mathbf{l}) = |\mathbf{l}|$ represent the momentum and energy of an exchanged gluon respectively.

REFERENCES

Fig. 1. Resolving Ambiguities in Current Matrix Elements.

Fig. 2. Diagrams Contributing to b_{eff} .

Fig .3. Diagrams Contributing to \mathcal{O}_{eff} .

Fig. 4. The Dynamical Quark Dispersion Relation. The solid line is the numerical result while the dashed line is the perturbative relation for $m(4 \text{ GeV}) = 3.1 \text{ MeV}$.

Fig. 5. The Chiral Condensate. The solid line is perturbation theory, the symbols represent the nonperturbative condensate for massless quarks (circles) and for $m(1 \text{ GeV}) = 5 \text{ MeV}$ (diamonds).